11º Workshop em Engenharia e Tecnologia Espaciais
18, 19 e 20 de agosto de 2020

Earth-Moon Transfer Between Elliptic Low Earth Orbit to Elliptic Low Moon Orbit in the Context of the Two-Body Problem

Luiz Arthur Gagg Filho [1], **Sandro da Silva Fernandes** [2]

[1] Instituto Tecnológico de Aeronáutica, São José dos Campos, SP, Brasil
Professor, Departamento de Mecânica do Voo.

[2]Instituto Tecnológico da Aeronáutica, São José dos Campos, SP, Brasil
Professor, Departamento de Matemática.

arthurga@ita.br

Abstract. *The present work determines bi-impulsive Earth-Moon trajectories of a space vehicle that departs from a prescribed elliptic low Earth orbit (LEO) and it arrives at an elliptic low Moon orbit (LMO). The eccentricity of the Moon orbit is considered, and, the Earth-Moon trajectory is formulated by using an elliptic patched-conic approximation. The terminal orbits are prescribed as well as the points of departure and arrival of the space vehicle in each terminal orbit. To solve this transfer problem, two-point boundary value problems are formulated. A two-degree of freedom optimization problem is also formulate to minimize the total fuel consumption. The results show that the trajectory with the smallest fuel consumption does not depart necessarily from the apsis of the LEO depending on the value of the pericenter argument of the LEO.*

Keywords: Earth-Moon mission; Optimal space trajectories; Elliptic patched-conic approximation; Elliptic terminal orbits.

1. Introduction

The majority of space mission use impulsive actuators for accomplishing orbit transfer maneuvers, including lunar and interplanetary missions. The impulsive propulsion system is characterized by a high thrust, like the chemical propulsion with a low specific impulse [Miele et al. 2004]. On the other hand, there is also the low thrust propulsion system like the electrical propulsion [Marec 1979] with high specific impulse. The space mission and the propulsion system reflect on the preliminary design of the space vehicle trajectory. Nowadays, there are several procedures to determine optimal impulsive (high thrust) and optimal low-thrust trajectories [Topputo et al. 2005]. Generally, optimization problems are not easy to solve in non-linear dynamics, which is the case of space missions; thus, a precise initial guess is commonly necessary. One can search the initial guess using complex models like the one based on ephemeris [Dei Tos and Topputo 2019]. However, simple models can also provide initial guess for the more complex non-linear dynamic model. In the context of the two-body problem (the simplest model for orbital maneuvers), one can determine trajectory approximations using several methods as: the Hohmann transfer [Hohmann 1960], the planar lunar patched-conic approximation [Gagg Filho and da Silva Fernandes 2015], the three-dimensional lunar patched-conic approximation [Gagg Filho and da Silva Fernandes 2016]. Therefore, one can add geometry complexity using only the context of the two-body allowing a more detail fuel consumption analysis in the preliminary mission design in a simple model.

The present work adds three geometry complexity in the planar lunar patched-conic approximation, which is also based on the two-body problem. The first one is to consider the eccentricity of the Moon orbit around the Earth. Despite the eccentricity of the Moon orbit be small, close to 0.0054, this value can influence the fuel consumption. Just for curiosity, the eccentric of Mercury orbit around the Sun is 0.2056. The others two geometry complexity are to consider the terminal orbits of the space mission also elliptic. So, in this work, the space vehicle departs from an elliptic low Earth (LEO) and it arrives in an elliptic low Moon orbit (LMO) by application of two impulsive velocity increments. The including of the eccentricity of the terminal orbits expands the range of applications of the preliminary analysis. On the Juno mission [Grammier 2006], for example, the space vehicle describes high eccentric orbits around Jupiter to avoid the strong magnetic field of this primary. The GARAEÉA-L brazilian mission [Fonseca and Nogueira 2016] intends to insert a probe into an elliptic orbit around the Moon. Therefore, this work generalizes the patched-conic geometry allowing the trajectory mission design for more applications and it provides initial guesses for more complex models.

2. Mathematical Modeling

The Earth-Moon transfer problem is enunciated as:

Problem 1 *Transfer a space vehicle from a prescribed low Earth orbit (LEO) to a prescribed low Moon orbit (LMO) by applying two velocity increments at prescribed points of these terminal orbits. It is assumed that the impulses are applied tangentially to the terminal orbits. The first velocity increment Δv_{LEO} inserts the space vehicle into a transfer trajectory, and, the second velocity increment Δv_{LMO} brakes the vehicle inserting it into the LMO. The terminal orbits and the Moon orbit are considered elliptic and co-planar, such that, the motion of the space vehicle lies on the plane of these orbits'. The fuel consumption is represented by the total characteristic velocity $\Delta v_{Total} = \Delta v_{LEO} + \Delta v_{LMO}$ [Marec 1979].*

In order to solve this problem, an elliptic patched-conic approximation is formulated as an extension of the classic lunar patched-conic approximation [Bate et al. 1971].

2.1. Elliptic patched-conic approximation

The patched-conic approximation utilizes the concept of Sphere of Influence to approximate the trajectory by linking ("patched") parts of conics, each of these corresponds to a two-body problem. For the Earth-Moon mission, the trajectory is approximated using two phases: the first one, a geocentric phase, characterizes an elliptical trajectory of the space vehicle subjected only to the gravitational field of the Earth; the second one, a selenocentric phase, characterizes an hyberbolic trajectory of the space vehicle subjected only to the gravitational field of the Moon (see Fig. 1). In this way, a first velocity increment Δv_{LEO}, applied at t_0 and tangential to the LEO, inserts the space vehicle into an elliptic geocentric phase departing from a given point at the LEO. This departure point is prescribed by its true anomaly $f_{LEO}(t_0)$. The selenocentric phase initiates when the space vehicle reaches the Moon's Sphere of Influence (SOI) at $t = t_1$, and, it terminates at t_f when the space vehicle reaches the prescribed point at the elliptic LMO, given by the true anomaly $f_{LMO}(t_f)$. At this moment, a second velocity increment Δv_{LMO} is applied to insert the space vehicle into the prescribed LMO. The angle λ_1 defines the geometry at the contact of the space vehicle with the Moon's SOI. Since the Moon orbit around Earth is elliptic, one must also prescribe the position of Moon on its orbit. One way to do that is to prescribe the eccentric anomaly of Moon $E_M(t_1)$ when the space vehicle reaches the Moon's SOI at t_1. Since the second velocity increment is supposed to be tangential to the LMO, the flight path angle φ_f on the selenocentric trajectory and the flight path angle φ_{LMO} on the LMO at t_f must be equal.

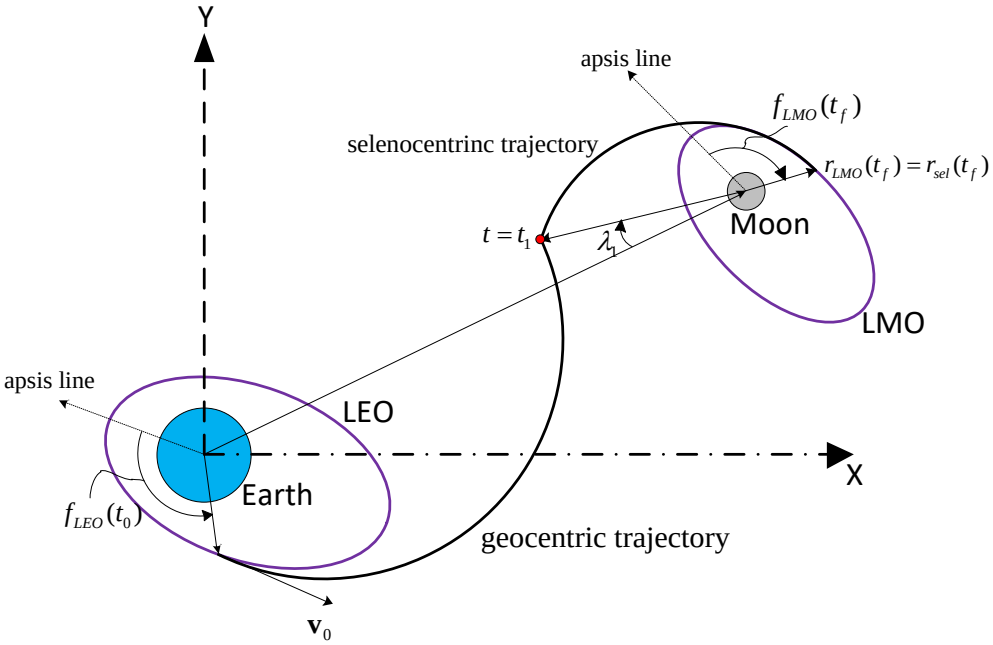

Figure 1. Elliptic patched-conic approximation for the Earth-Moon transfer.

In this way, the following two-point boundary value problem is enunciated:

Problem 2 *Given the values of* λ_1, $f_{LEO}(t_0)$, $f_{LMO}(t_f)$, $E_M(t_1)$, *and, prescribing the semi-major axis and eccentricity of the terminal orbits (or, equivalently, the apocenter and pericenter distances), determine the initial velocity* v_0 *of the space vehicle immediately after the application of the first velocity increment in order to satisfy the final constraint:*

$$g\,(v_0): \quad r_{sel}(t_f) - r_{LMO}(t_f) = 0 \tag{1}$$

where $r_{sel}(t_f)$ is the distance from the Moon to the space vehicle at t_f calculated using the well-known two-body problem expressions for the hyperbolic selenocentric trajectory. The calculation of $r_{sel}(t_f)$ supposes that $\varphi_f = \varphi_{LMO}$ since the hyperbolic selenocentric trajectory must be tangential to the LMO at the prescribed point described by $f_{LMO}(t_f)$ (see Fig. 1); and, $r_{LMO}(t_f)$ is the distance from the Moon to the space vehicle calculated by using the two-body expressions for the elliptic LMO with the prescribed value of $f_{LMO}(t_f)$. Observe that the pericenter argument ω_{LMO} of the LMO must not be prescribed because it is part of the solution.

Note that in Problem 2, the variable λ_1 is prescribed. This variable is directly related to the pericenter argument ω_{LEO} of the LEO, which must me calculated after the problem is solved. Therefore, prescribing λ_1 and $f_{LEO}(t_0)$ is equivalent to prescribe the initial phase angle of the space vehicle at departure from the LEO. On the other hand, one can enunciate a variant of this problem by prescribing ω_{LEO} instead of λ_1 as:

Problem 3 *Given the values of* ω_{LEO}, $f_{LEO}(t_0)$, $f_{LMO}(t_f)$, $E_M(t_1)$, *and, prescribing the semi-major axis and eccentricity of the terminal orbits (or, equivalently, the apocenter and pericenter*

distances), determine the initial velocity v_0 of the space vehicle immediately after the application of the first velocity increment in order to satisfy the final constraint:

$$g\left(v_0\right): \quad r_{sel}(t_f) - r_{LMO}(t_f) = 0 \tag{2}$$

Another possibility is to set λ_1 as an unknown to be determined. Moreover, the eccentric anomaly of the Moon $E_M(t_1)$, generally, is not part of the mission design. So, in order to set both λ_1 and $E_M(t_1)$ as unknowns, one can formulate a two-degree of freedom optimization problem as it follows:

Problem 4 *Given the values of $f_{LEO}(t_0)$, $f_{LMO}(t_f)$, and, prescribing the semi-major axis and eccentricity of the terminal orbits (or, equivalently, the apocenter and pericenter distances), determine the initial velocity v_0 of the space vehicle immediately after the application of the first velocity increment in order to minimize the total fuel consumption given by :*

$$F\left(v_0, \lambda_1, E_M(t_1)\right) : \Delta v_{Total} = \Delta v_{LEO} + \Delta v_{LMO} \tag{3}$$

subjected to the following constraint

$$g\left(v_0, \lambda_1, E_M(t_1)\right): \quad r_{sel}(t_f) - r_{LMO}(t_f) = 0 \tag{4}$$

3. Results

This section is divided in two parts. The first one solves the TPBVP associated to the Problem 3 for several values of $f_{LEO}(t_0)$ and ω_{LEO}. The Newton-Raphson method [Press et al. 1997] is implemented in FORTRAN to solve this problem. The second part analyses the results of the optimization problem associated to the Problem 4, in which $f_{LEO}(t_0)$ and ω_{LEO} are set as unknowns. The Sequential Gradient Restoration Algorithm [Miele et al. 1969] is also implemented in FORTRAN to solve this optimization problem. Table 1 shows the main physical parameters of the problem.

Table 2 highlights the values of the variables that must be prescribed in Problem 3. The LMO pericenter altitude and the LMO apocenter altitude are the same of the GARATEA-L mission [Fonseca and Nogueira 2016]. Combinations of values of $f_{LEO}(t_0)$ and ω_{LEO} are set by prescribing both variables within the interval $[0°, 360°]$ with discretization of $1°$.

Table 1. Physical parameters.

Earth's radius	6378.2 km
Moon's radius	1738 km
Earth's gravitational parameter	398600 km^3/s^2
Moon's gravitational parameter	4902.83 km^3/s^2
Moon SOI radius	66300 km

Figure 2 plots the regions of solution considering the combinations of $f_{LEO}(t_0)$ and ω_{LEO}. Note in this figure that there is a small portion of feasible solutions. This occurs because there is a

Table 2. Mission parameters for the TPBVP.

LEO pericenter altitude	167 km
LEO apocenter altitude	1670 km
LMO pericenter altitude	300 km
LMO apocenter altitude	1000 km
$E_M(t_1)$	160°
$f_{LMO}(t_f)$	0°

limited interval of the initial phase angle, which is given by $\theta_{EP}(0) = f_{LEO}(t_0) + \omega_{LEO}$ for a counterclockwise LEO, that solves the direct ascent maneuver. If the geocentric leg of the transfer trajectory does not intercept the Moon's SOI, the solution does not exist. Figure 3 plots the Δv_{Total} against $\theta_{EP}(0) = f_{LEO}(t_0) + \omega_{LEO}$ showing that the solutions are confined in a small interval of $\theta_{EP}(0)$.

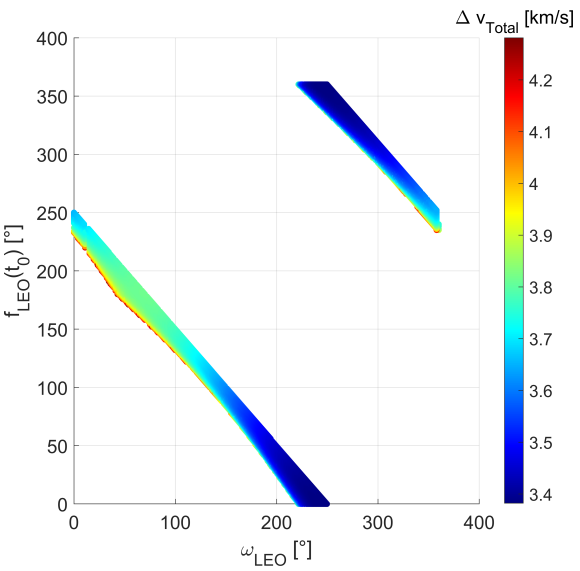

Figure 2. Solution regions of the TPBVP (Problem 3) for several $f_{LEO}(t_0)$ and ω_{LEO}.

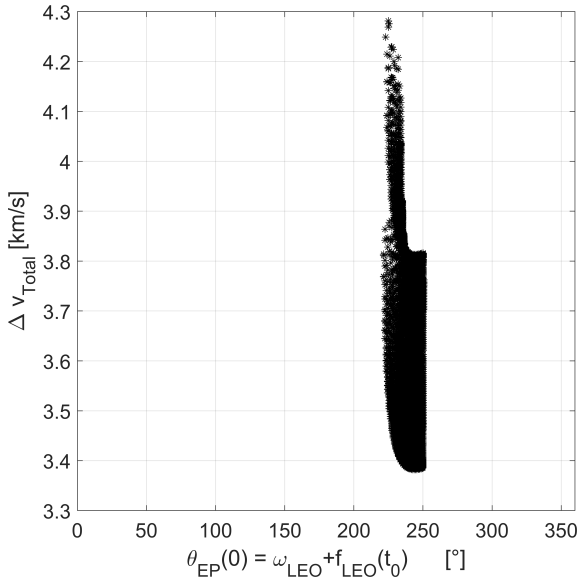

Figure 3. Fuel consumption $\times$ $\theta_{EP}(0)$.

Figure 4 considers solutions with highlighted values of ω_{LEO} and Figure 5 is an extension of Fig 4 with all the values of ω_{LEO}. Observe that, for a given value of $f_{LEO}(t_0)$ there is a value of ω_{LEO} that reaches the minimum Δv_{Total}. Similarly, given a value of ω_{LEO}, there is a value of $f_{LEO}(t_0)$, which is not necessarily 0°, that reaches a minimum Δv_{Total}; thus, the envelope, originated by the solutions on Fig. 5, provides the mininum fuel consumption solutions for a given value of ω_{LEO}. The minimum of this envelope provides the smallest fuel consumption trajectory of all minimum solutions. This smallest fuel consumption trajectory of Fig. 5 is depicted on Figs. 6 – 8 for $E_M(t_1) = 160°$ and the results are shown in Tab. 3. The geometry at departure is better visualized on Fig. 7, in which the orientation of the apsis line of the LEO, i.e., the value of ω_{LEO} is prescribed indirectly by the angle λ_1. Figure 8 better illustrates the arrival geometry, in which the orientation of the apsis line of the LMO, i.e., the value of the ω_{LMO}, is determined after solving Problem 2.

Note that, for the smallest fuel consumption the true anomaly on the terminal orbits must be 0°. In order to precisely obtain the minimum fuel consumption trajectory for a given ω_{LEO}, a

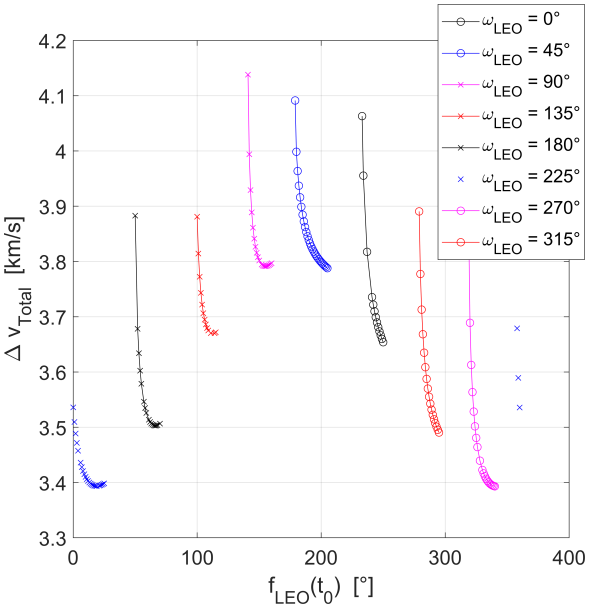

Figure 4. Solutions of the Problem 3 for some prescribed values of ω_{LEO}.

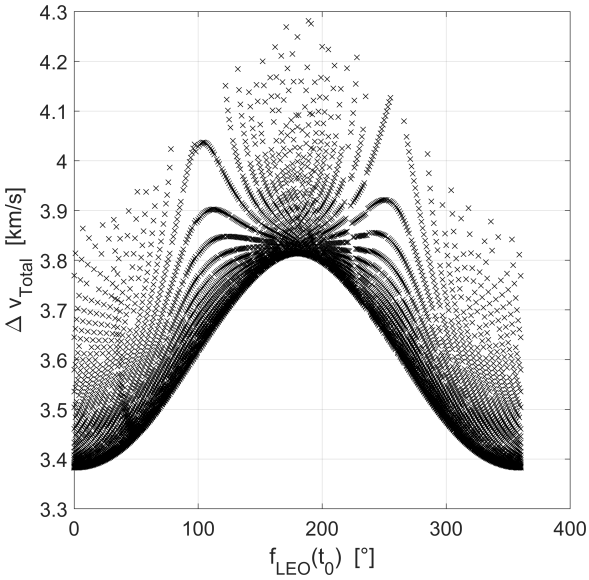

Figure 5. Solutions of the Problem 3 for all values of ω_{LEO}.

simple method based on the gradient can be applied to solve the optimization problem, since the curve to be optimized is smooth (see, for instance, the curve with $\omega_{LEO} = 90°$ in Fig. 4).

Table 3. Main parameters of the smallest fuel consumption trajectory.

ω_{LEO}	243.637°
$f_{LEO}(t_0)$	0°
Δv_{LEO}	2.750935 km/s
Δv_{LMO}	0.631222 km/s
Δv_{Total}	3.382157 km/s
$Time$	5.120 days
λ_1	72.801°

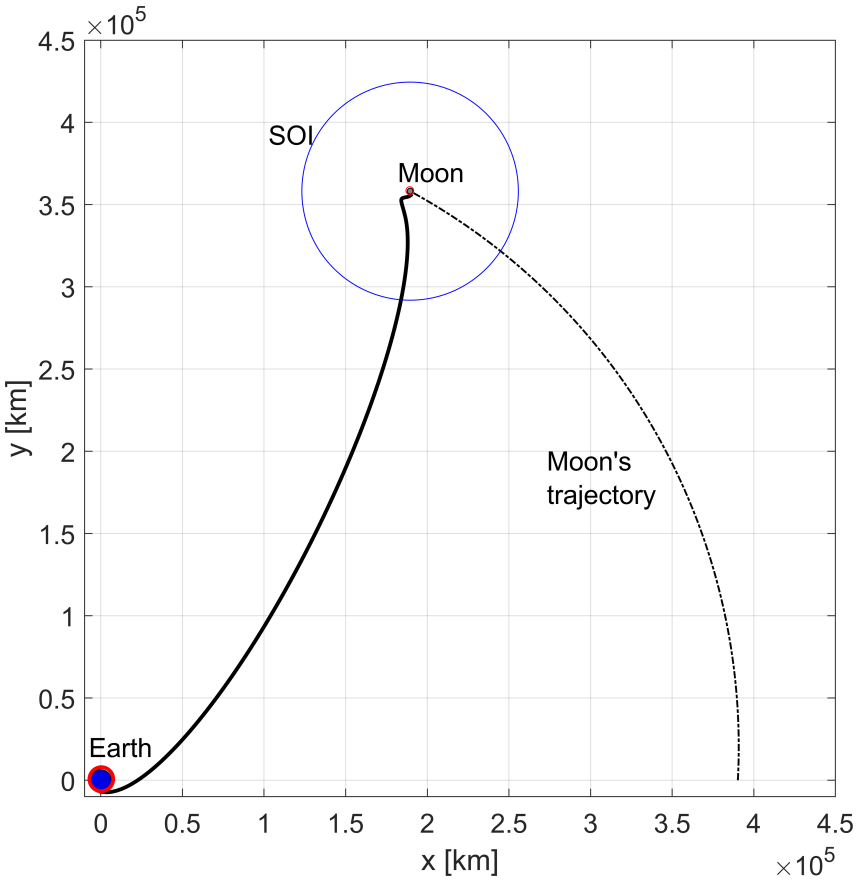

Figure 6. Smallest fuel consumption trajectory for $E_M(t_1) = 160°$. Complete trajectory.

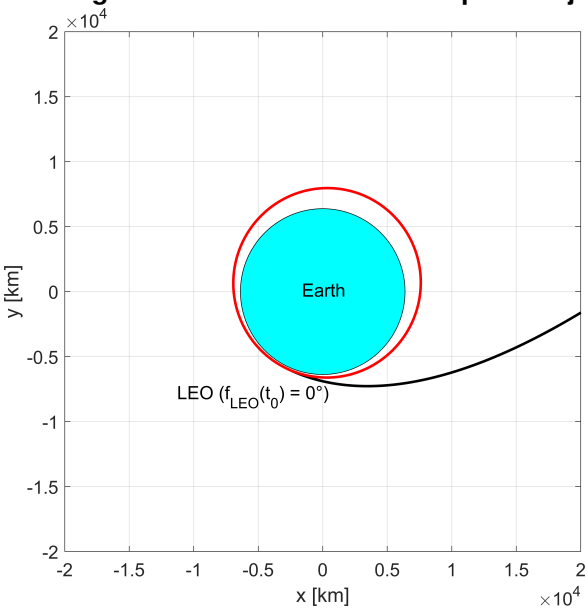

Figure 7. Smallest fuel consumption trajectory for $E_M(t_1) = 160°$. Departing trajectory.

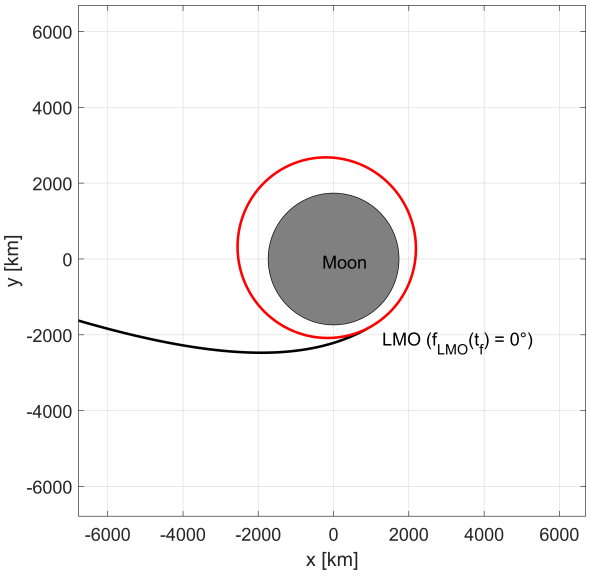

Figure 8. Smallest fuel consumption trajectory for $E_M(t_1) = 160°$. Arrival trajectory.

Problem 4 is used to solve the optimization problem, in which the variables λ_1 (or, equivalently, ω_{LEO}) and $E_M(t_1)$ are set as unknowns to be optimized. The LMO pericenter altitude and the LMO apocenter altitude for this optimization problem are set, respectively, 100 km and 300 km. Figures 9 and 10 shows the solution regions considering combinations of prescribed values $f_{LEO}(t_0)$ and $f_{LMO}(t_f)$ within the interval $[0°, 360°]$ with discretization of $1°$ for both variables. As one can see, given a value of $f_{LEO}(t_0)$, the fuel consumption of the optimal solutions decreases as the $f_{LMO}(t_f)$ approximates to $0°$ (Fig. 9). For instance, note that the iso-fuel consumption curve with $\Delta v_{Total} = 3.78 km/s$ turns to the left with the increasing of $f_{LMO}(t_f)$; so, for the given $f_{LEO}(t_0) = 100°$, the smallest fuel consumption of all optimal trajectories is on the beginning of this iso-fuel consumption curve, which corresponds to f_{LMO} near to $0°$. In order to determine the precise value of $f_{LMO}(t_f)$, a three-degree of freedom optimization problem must be solved. The optimal values of the initial phase angle of the space vehicle $\theta_{EP}(0)$ and the optimal values of the Moon's position $E_M(t_1)$ do not have greater changes (Fig. 10) with the prescribing values of $f_{LEO}(t_0)$ and $f_{LMO}(t_f)$.

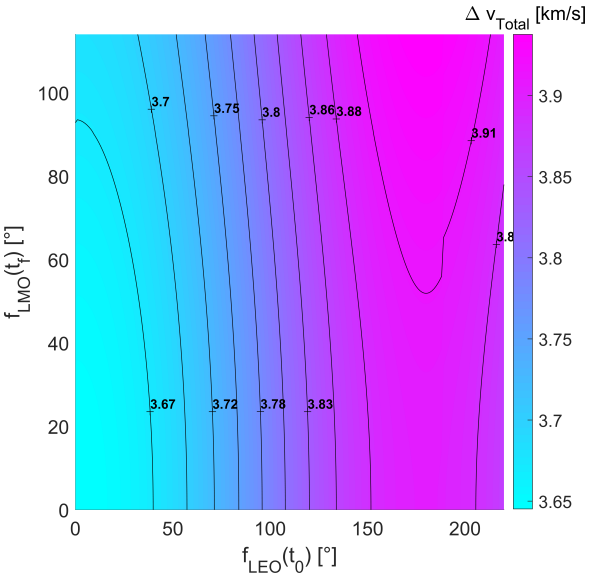

Figure 9. Solutions for the two-degree of freedom optimization problem (Problem 4). $f_{LEO}(t_0)$ **and** $f_{LMO}(t_f)$ **are prescribed.** $f_{LEO}(0) \times f_{LEO}(t_f)$**.**

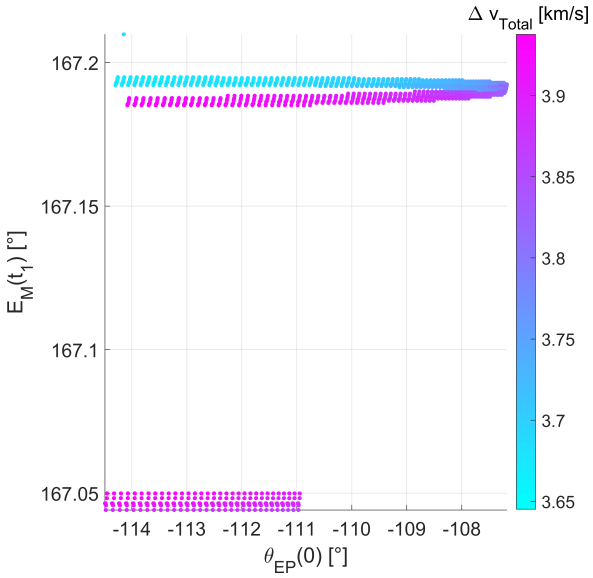

Figure 10. Solutions for the two-degree of freedom optimization problem (Problem 4). $f_{LEO}(t_0)$ **and** $f_{LMO}(t_f)$ **are prescribed.** $\theta_{EP}(0) \times E_M(t_1)$**.**

4. Conclusion

The present work determines optimal bi-impulsive Earth-Moon trajectories by extending the classic lunar patched-conic approximation, which is based on the two-body problem. The formulated new patched-conic approximation considers the eccentricity of the Moon's orbit around the Earth and the eccentricities of the terminal orbits (LEO and the LMO), thus allowing the departure and the arrival of the space vehicle at any part of the elliptic terminal orbit, i.e., the Earth-Moon transfer is not necessarily between the apsis. To solve this patched-conic approximation, two-point boundary value problems are enunciated in which a phase angle of the space vehicle ($\theta_{EP}(0)$ or λ_1) and the position of the Moon on its orbits must be prescribed. A two-degree of freedom optimization problem is also enunciated in which the phase angle of the space vehicle and the position of the Moon on its orbit are set as unknowns to be determined in order to minimize the total fuel consumption.

The results show that depending on the value of the pericenter argument of the LEO, the minimum fuel consumption trajectory does not departs necessarily at the pericenter. On the other hand, for a prescribed value of the true anomaly of the LEO at departure, the minimum fuel consumption trajectory lies on a specific value of the LEO pericenter argument. The results of the two-degree optimization problem reveals that the optimal value of the position of the Moon on its orbits, given by an eccentric anomaly, and the optimal value of the initial phase angle of the space vehicle are nearly independent with the prescribed values of the true anomalies at departure and arrival of the LEO and LMO respectively.

Bibliografy

Bate, R. R., Mueller, D. D., and White, J. E. (1971). *Fundamentals of astrodynamics*. Courier Dover Publications, New York.

Dei Tos, D. A. and Topputo, F. (2019). High-Fidelity Trajectory Optimization with Application to Saddle-Point Transfers. *Journal of Guidance, Control, and Dynamics*, 42(6):1343–1352.

Fonseca, L. and Nogueira, S. (2016). A missão.

Gagg Filho, L. A. and da Silva Fernandes, S. (2015). Optimal round trip lunar missions based on the patched-conic approximation. *Computational and Applied Mathematics*, pages 1–35.

Gagg Filho, L. A. and da Silva Fernandes, S. (2016). Finding the Optimal Spatial Geometry in an Earth-Moon Mission. In *Proceedings...*, Reston. AIAA/AAS Astrodynamics Specialist Conference, AIAA.

Grammier, R. S. (2006). An overview of the Juno Mission to Jupiter. *25th International Symposium on Space Technology & Science*, pages 1–9.

Hohmann, W. (1960). The attainability of heavenly bodies. *NASA Technical Translation F-44*.

Marec, J.-P. (1979). *Optimal space trajectories*. Elsevier, New York, NY.

Miele, A., Huang, H. Y., and Heideman, J. C. (1969). Sequential gradient-restoration algorithm for the minimization of constrained functions–Ordinary and conjugate gradient versions. *Journal of Optimization Theory and Applications*, 4(4):213–243.

Miele, A., Wang, T., and Williams, P. N. (2004). Computation of optimal Mars trajectories via combined chemical/electrical propulsion, part 1: baseline solutions for deep interplanetary space. *Acta Astronautica*, 55(2):95–107.

Press, W. H., Teukolsky, S. A., Vetterling, W. T., and Flannery, B. P. (1997). Numerical Recipes in Fortran 77: the art of scientific computing, ch. 14.8. In *Numerical Recipies in Fortran 77*.

Topputo, F., Vasile, M., and Bernelli-Zazzera, F. (2005). Low energy interplanetary transfers exploiting invariant manifolds of the restricted three-body problem. *Journal of the Astronautical Sciences*, 53(4):353–372.